Whole-exome sequencing identifies mutations in *FSIP2* as a recurrent cause of multiple morphological abnormalities of the sperm flagella

Guillaume Martinez[1,2], Zine-Eddine Kherraf[1,3], Raoudha Zouari[4], Selima Fourati Ben Mustapha[4], Antoine Saut[1,2], Karin Pernet-Gallay[5], Anne Bertrand[5], Marie Bidart[6], Jean Pascal Hograindleur[1], Amir Amiri-Yekta[1,6,7], Mahmoud Kharouf[4], Thomas Karaouzène[1,8], Nicolas Thierry-Mieg[8], Denis Dacheux-Deschamps[9,10], Véronique Satre[1,2], Mélanie Bonhivers[9,10], Aminata Touré[11,12,13], Christophe Arnoult[1], Pierre F. Ray[1,3,*,†], and Charles Coutton[1,2,†]

[1]University Grenoble Alpes, INSERM U1209, CNRS UMR 5309, Institute for Advanced Biosciences, Team Genetics Epigenetics and Therapies of Infertility, 38000 Grenoble, France [2]CHU Grenoble Alpes, UM de Génétique Chromosomique, Grenoble, France [3]CHU de Grenoble, UM GI-DPI, Grenoble F-38000, France [4]Clinique des Jasmins, 23, Av. Louis BRAILLE 1002 Belvedere, Tunis, Tunisia [5]Grenoble Neuroscience Institute, INSERM 1216, Grenoble F38000, France [6]CHU Grenoble Alpes, UM de Biochimie Génétique et Moléculaire, Grenoble, France [7]Department of Genetics, Reproductive Biomedicine Research Center, Royan Institute for Reproductive Biomedicine, ACECR, Tehran, Iran [8]University Grenoble Alpes/CNRS, TIMC-IMAG, F-38000 Grenoble, France [9]Université de Bordeaux, Microbiologie Fondamentale et Pathogénicité, CNRS UMR 5234, Bordeaux, France [10]Institut Polytechnique de Bordeaux, Microbiologie Fondamentale et Pathogénicité, UMR-CNRS 5234, F-33000 Bordeaux, France [11]INSERM U1016, Institut Cochin, Paris 75014, France [12]Centre National de la Recherche Scientifique UMR8104, Paris 75014, France [13]Faculté de Médecine, Université Paris Descartes, Sorbonne Paris Cité, Paris 75014, France

*Correspondence address. UM GI-DPI, IBP, CHU Grenoble Alpes, 38043 Grenoble Cedex 9, France. Tel: +33-4-76-76-55-73; E-mail: pray@chu-grenoble.fr

STUDY QUESTION: Can whole-exome sequencing (WES) of infertile patients identify new genes responsible for multiple morphological abnormalities of the sperm flagella (MMAF)?

SUMMARY ANSWER: WES analysis of 78 infertile men with a MMAF phenotype permitted the identification of four homozygous mutations in the fibrous sheath (FS) interacting protein 2 (*FSIP2*) gene in four unrelated individuals.

WHAT IS KNOWN ALREADY: The use of high-throughput sequencing techniques revealed that mutations in the dynein axonemal heavy chain 1 (*DNAH1*) gene, and in the cilia and flagella associated protein 43 (*CFAP43*) and 44 (*CFAP44*) genes account for approximately one-third of MMAF cases thus indicating that other relevant genes await identification.

STUDY DESIGN, SIZE, DURATION: This was a retrospective genetics study of 78 patients presenting a MMAF phenotype who were recruited in three fertility clinics between 2008 and 2015. Control sperm samples were obtained from normospermic donors. Allelic frequency for control subjects was derived from large public databases.

PARTICIPANTS/MATERIALS, SETTING, METHODS: WES was performed for all 78 subjects. All identified variants were confirmed by Sanger sequencing. Relative mRNA expression levels for the selected candidate gene (*FSIP2*) was assessed by quantitative RT-PCR in a panel of normal human and mouse tissues. To characterize the structural and ultrastructural anomalies present in patients' sperm,

---

[†]Equal contribution, the authors should both be regarded as last authors.

---

immunofluorescence (IF) was performed on sperm samples from two subjects with a mutation and one control and transmission electron microscopy (TEM) analyses was performed on sperm samples from one subject with a mutation and one control.

MAIN RESULTS AND THE ROLE OF CHANCE: We identified four unrelated patients (4/78, 5.1%) with homozygous loss of function mutations in the *FSIP2* gene, which encodes a protein of the sperm FS and is specifically expressed in human and mouse testis. None of these mutations were reported in control sequence databases. TEM analyses showed a complete disorganization of the FS associated with axonemal defects. IF analyses confirmed that the central-pair microtubules and the inner and outer dynein arms of the axoneme were abnormal in all four patients carrying *FSIP2* mutations. Importantly, and in contrast to what was observed in patients with MMAF and mutations in other MMAF-related genes (*DNAH1*, *CFAP43* and *CFAP44*), mutations in *FSIP2* led to the absence of A-kinase anchoring protein 4 (AKAP4).

LIMITATIONS, REASONS FOR CAUTION: The low number of biological samples and the absence of a reliable anti-FSIP2 antibody prevented the formal demonstration that the FSIP2 protein was absent in sperm from subjects with a *FSIP2* mutation.

WIDER IMPLICATIONS OF THE FINDINGS: Our findings indicate that *FSIP2* is one of the main genes involved in MMAF syndrome. In humans, genes previously associated with a MMAF phenotype encoded axonemal-associated proteins (*DNAH1*, *CFAP43* and *CFAP44*). We show here that FSIP2, a protein of the sperm FS, is also logically associated with MMAF syndrome as we showed that it is necessary for FS assembly and for the overall axonemal and flagellar biogenesis. As was suggested before in mouse and man, our results also suggest that defects in AKAP4, one of the main proteins interacting with FSIP2, would induce a MMAF phenotype. Finally, this work reinforces the demonstration that WES sequencing is a good strategy to reach a genetic diagnosis for patients with severe male infertility phenotypes.

Introduction

Teratozoospermia, a condition defined by the presence of sperm with abnormal morphology, comprises a large variety of phenotypes, many of which are among the most severe infertility phenotypes in human (Coutton *et al.*, 2015). Patients with severe flagellar defects, and most strikingly presenting a much reduced flagellar length, have been described in numerous studies, and as 'dysplasia of the fibrous sheath (DFS)', 'short tails' or 'stump tails' (Chemes *et al.*, 1987, 2000; Rawe *et al.*, 2001; Chemes and Rawe, 2003). In our experience these patients do not present a homogeneous phenotype of short flagella but exhibit various flagellar abnormalities including absent, short, coiled, bent and irregular flagella (for illustration see Fig. 1). We therefore proposed to reclassify this heterogeneous phenotype comprising multiple morphological abnormalities of the sperm flagella (MMAF) for

patients with a severe asthenozoospermia and with more than 5% of sperm showing at least four of the five aforementioned flagellar anomalies (Ben Khelifa *et al.*, 2014). As the fibrous sheath (FS) is an internal structure of the flagella, detection of its anomalies (dysplasia) can only be achieved by ultrastructural observation of the flagella by electron microscopy (EM). As such studies are not performed in the routine setting, we did not feel that this designation was practical. The DFS appellation is however interesting as such anomalies are not always marked in sperm from MMAF patients, and DFS therefore likely represents a MMAF ultrastructural phenotype highlighting anomalies pertaining to this specific structure (see discussion in Coutton *et al.*, 2015; Ray *et al.*, 2017). In this article the generic term MMAF is normally used but we also use the term DFS when referring to subjects who have clearly been classified as DSF upon EM examination.
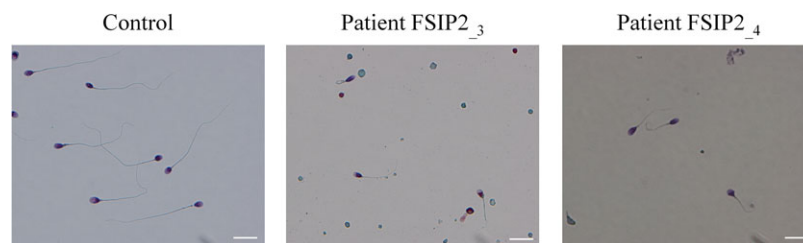

Figure 1 Morphology of spermatozoa from two patients with a mutation in the *FSIP2* gene. All spermatozoa from patients FSIP2_3 and FSIP2_4 have shorter flagella than controls with no mutation in the fibrous sheath interacting protein 2 (*FSIP2*) gene. Additional features of spermatozoa from men with the multiple morphological abnormalities of the sperm flagella (MMAF) phenotype, such as thick and coiled flagella, are also observed. Scale bars 10 μm.

Mutations in *DNAH1*, *CFAP43*, *CFAP44* and in cilia and flagella associated protein 69 (*CFAP69*) have recently been reported to be recurrent genetic causes of MMAF in human, highlighting the genetic heterogeneity of this phenotype (Ben Khelifa *et al.*, 2014; Amiri-Yekta *et al.*, 2016; Sha *et al.*, 2017; Tang *et al.*, 2017; Coutton *et al.*, 2018; Dong *et al.*, 2018). These genes encode different components of the axoneme, a highly conserved central cytoskeletal structure shared by both the sperm flagellum and other motile cilia (Inaba, 2007; Satir and Christensen, 2008). In mouse models, in addition to axonemal genes, mutations in several genes coding for accessory structures of the flagellum have also been associated with sperm tail defects (Lehti and Sironen, 2017). Interestingly, a first genetic diagnosis was proposed 12 years ago for a patient described with DFS. He presented with a deletion removing part of A-kinase anchoring protein 3 (*AKAP3*) and *AKAP4*, two genes encoding proteins of the sperm FS (Baccetti *et al.*, 2005), one of the main peri-axonemal structures surrounding the flagellum axoneme (Inaba, 2003, 2011). However, no other mutations in *AKAP* genes or in any other FS-related genes have been reported since this initial description of an *AKAP3/4* deletion (Turner *et al.*, 2001; Coutton *et al.*, 2015; Ray *et al.*, 2017). More than 20 proteins are estimated to be located in, or closely associated with, the FS of mammalian spermatozoa and FSIP2 is believed to be a major structural protein of the FS (Eddy, 2007). Altogether, these proteins are involved in the control of sperm flagellum elasticity, glycolytic activities and phosphorylation signaling pathways that regulate sperm motility (Miki *et al.*, 2002; Eddy, 2007; Inaba, 2011).

Previous genetic analysis of a large cohort of 78 infertile patients with MMAF permitted the identification of a total of 22 patients with mutations in *DNAH1*, *CFAP43* and *CFAP44* (Coutton *et al.*, 2018). Here we re-analyzed the genetic data obtained by whole-exome sequencing (WES) from the 56 (out of 78) non-diagnosed patients and identified four unrelated subjects carrying bi-allelic loss of function mutations in *FSIP2*, which encodes a FS protein interacting with AKAP4 (Brown *et al.*, 2003). Importantly, we observed in *FSIP2*-mutated individuals that the AKAP4 protein was absent from all spermatozoa; a feature which was not observed in spermatozoa from other MMAF individuals of different genetic etiology. Overall, our work confirms what has been suggested long ago: that not only axonemal components, but also peri-axonemal proteins from the FS play an important role in the assembly and/or the stability of the axoneme (Escalier and David, 1984; Chemes *et al.*, 1987, 1998) and that genetic defects interfering with the competent synthesis of these proteins induce a MMAF phenotype.

Materials and Methods

Subjects and controls

All patients presented with a typical MMAF phenotype defined by asthenozoospermia (total motility <40%) with >5% of at least three flagellar morphological abnormalities (absent, short, coiled, bent and irregular flagella). The four FSIP2 patients (FSIP2_1 to FSIP2_4) originated from North Africa (Tunisians) and were treated in Tunis at the Clinique des Jasmins for primary infertility from 2008 to 2015. The four patients had normal somatic karyotypes 46,XY and were negative for Y chromosome microdeletions. These four patients were born from related parents, generally first cousins. Sperm analysis was carried out in the source laboratory during the course of the routine biological examination of the patient, according to World

Health Organization guidelines (Wang *et al.*, 2014). Written informed consent for genetic testing was obtained from all the subjects participating in the study according to the local protocols and the principles of the Declaration of Helsinki. Sperm samples permitting additional analyses (IF and EM) were only available from patients FSIP2_3 and FSIP2_4. In addition, the study was approved by local ethic committees. The samples were stored in the center for biological resources (CRB) Germetheque (certification under ISO-9001 and NF-S 96-900) following a standardized procedure. Control samples from fertile individuals with normal spermograms were obtained from CRB Germetheque. Consent for CRB storage was approved by the CPCP Sud-Ouest of Toulouse (co-ordination of the multisites CRB Germetheque).

WES and bioinformatics analysis

WES was performed according to our protocol described in Coutton *et al.* (2018). The main difference with the initial analysis was that we used an updated version of GATK and analyzed the variants which had been initially marked as variants of poor confidence. Briefly, genomic DNA was isolated from saliva using an Oragen DNA extraction kit (DNAgenotech®, Ottawa, Canada). Coding regions and intron/exon boundaries were enriched using the 'all Exon V5 kit' (Agilent Technologies, Wokingham, UK). DNA sequencing was undertaken at the Genoscope, Evry, France, on the HiSeq 2000 from Illumina® (San Diego, CA, USA). Sequence reads were aligned to the reference genome (hg19) using MAGIC (SEQC/MAQC-III Consortium, 2014). MAGIC produces quality-adjusted variant and reference read counts on each strand at every covered position in the genome. Duplicate reads and reads that mapped to multiple locations in the genome were excluded from further analysis. Positions where sequence coverage was below 10 on either the forward or reverse strand were marked as low confidence, and positions with coverage below 10 on both strands were excluded. Single nucleotide variations (SNV) and small insertions/deletions (indels) were identified and quality-filtered using in-house scripts, which included part of the Genome Analysis Toolkit (GATK 3.7). Briefly, for each variant, independent calls are made on each strand, and only those positions where both calls agreed were retained. The candidate variants were identified using an in-house bioinformatics pipeline, as follows. Variants with a minor allele frequency >5% in the NHLBI ESP6500 [Exome Variant Server, NHLBI GO Exome Sequencing Project (ESP), Seattle, WA, USA] or in 1000 Genomes Project phase 1 datasets (1000 Genomes Project Consortium *et al.*, 2012), or >1% in ExAC (Lek *et al.*, 2016) or gnomAD (http://gnomad.broadinstitute.org/) were discarded. We also compared these variants to an in-house database of 94 control exomes obtained from subjects mainly originating from North Africa and the Middle East, corresponding to the geographical origin of most patients from this study and which are under-represented in single nucleotide polymorphism public databases. All variants present in a homozygous state in this database were excluded. We used Variant Effect Predictor (VEP version 81 (McLaren *et al.*, 2016)) to predict the impact of the selected variants. We only retained variants impacting splice donor/acceptor or causing frameshift, inframe insertions/deletions, stop gain, stop loss or missense variants, except those scored as 'tolerated' by SIFT (Kumar *et al.*, 2009) (sift.jcvi.org) and as 'benign' by Polyphen-2 (Adzhubei *et al.*, 2010) (genetics.bwh.harvard.edu/pph2).

Sanger sequencing

FSIP2 mutations identified by WES were validated by Sanger sequencing in each patient. The PCR primers and protocols used for each patient are listed in Supplementary Table SI. Sequencing reactions were carried out with BigDye Terminator v3.1 (Applied Biosystems) and were run on an ABI 3130XL system (Applied Biosystems™, ThemoFisher Scientific,

Waltham, MA, USA). Sequences were analyzed using SeqScape software (Applied Biosystems).

Quantitative real-time RT-PCR analysis

Quantitative real-time RT-PCR (RT-qPCR) was performed with cDNAs from various tissues of human and mouse, including testes (Amsbio, Abingdon, UK). A panel of seven organs was used for the experiments: testis, brain, lung, kidney, liver, colon and heart. Each sample was assayed in triplicate for each gene on a StepOnePlus (Life Technologies® ThemoFisher Scientific), with Power SYBR®Green PCR Master Mix (Life Technologies®). The PCR cycle was as follows: 10 min at 95°C, 1 cycle for enzyme activation; 15 s at 95°C, 60 s at 60°C with fluorescence acquisition, and 40 cycles for the PCR. RT-qPCR data were normalized using the reference housekeeping actin beta gene (*ACTB*) for human with the $-\Delta\Delta$Ct method (Livak and Schmittgen, 2001). The $2-\Delta\Delta$Ct value was set at 0 in brain cells, resulting in an arbitrary expression of 1. Primer sequences and RT-qPCR conditions are indicated in Supplementary Table SII. The efficacy of primers was checked using a standard curve. Melting curve analysis was used to confirm the presence of a single PCR product.

Statistical analysis was performed using a two-tailed Student's *t*-test on Prism 4.0 software (GraphPad, San Diego, CA, USA) to compare the relative expression of *FSIP2* transcripts in several organs. Statistical tests with a two-tailed *P* values ≤ 0.05 were considered significant.

Immunostaining in human sperm cells

Immunofluorescence (IF) staining were performed using sperm cells from control individuals, patients FSIP2_3 and FSIP2_4 and MMAF patients mutated in *CFAP43* and *CFAP44* and *DNAH1*. Sperm cells were fixed in PBS/4% paraformaldehyde for 1 min at room temperature. After washing in 1 ml PBS, the sperm suspension was spotted onto 0.1% poly L-lysine pre-coated slides (Thermo Scientific, ThemoFisher Scientific). After attachment, sperm were washed and permeabilized with 0.1% (v/v) Triton X-100—Dulbecco's phosphate-buffered saline (Triton X-100; Sigma-Aldrich St. Louis MO, USA.) for 30 min at room temperature. Slides were then blocked in 2% corresponding normal serum–DPBS (normal goat or donkey serum; GIBCO, Invitrogen, Carlsbad, CA, USA) and incubated overnight at 4°C with primary antibodies. Washes were performed with 0.1% (v/v) Triton X-100–DPBS, followed by 90 min incubation at room temperature with secondary antibodies. Appropriate controls were performed, omitting the primary antibodies. Samples were counterstained with 2 µg/ml DAPI (Sigma-Aldrich) and mounted with DAKO mounting media (Life Technology, ThemoFisher Scientific). Fluorescence images were captured with a Zeiss LSM 710 confocal microscope (Carl Zeiss, Oberkochen, Germany). Primary antibodies: polyclonal rabbit anti-AKAP4 (HPA020046, Sigma-Aldrich, 1:100), rabbit polyclonal anti-sperm associated antigen 6 (SPAG6) (HPA038440, Sigma-Aldrich, 1:500), rabbit polyclonal anti-dynein axonemal heavy chain 5 (DNAH5) (HPA037470, Sigma-Aldrich, 1:100), rabbit polyclonal anti-dynein axonemal light intermediate chain 1 (DNALI1) (HPA028305, Sigma-Aldrich, 1:100), mouse monoclonal anti-heat shock protein 60 (HSP60) (ab13532, 1:500, Abcam, Cambridge UK), monoclonal mouse anti-acetylated-α-tubulin (T7451, Sigma-Aldrich, 1:2000). Secondary antibodies: Highly cross-adsorbed secondary antibodies Dylight 488 and Dylight 549 (1:1000, Jackson Immunoresearch®; Ely, UK).

Transmission EM of human sperm cells

We performed transmission EM (TEM) experiments using sperm cells from fertile control individuals and from patient FSIP2_4 carrying the homozygous variant c.16389_16392delAATA in *FSIP2*. Sperm cells were fixed

with 2.5% glutaraldehyde and 2% formaldehyde in 0.1 M sodium phosphate (pH 7.4) for 2 h at room temperature. Cells were washed with phosphate buffer and post fixed with 1% osmium tetroxide in the same buffer for 1 h at 4°C. After washing with distilled water, cells were stained overnight at 4°C with 0.5% uranyl acetate pH 4.0. Cells were dehydrated through graded alcohols (30, 60, 90, 100, 100 and 100%; 10 min for each bath) and infiltrated with a mix of 1:1 Epon/alcohol 100% for 2 h before two washes in fresh Epon for 2 h. Finally, cells were immersed in fresh Epon and polymerized for 2 days at 60°C. Ultrathin sections of the cell pellet were prepared with an ultramicrotome (Leica Wetzlar, Germany). Sections were post-stained for 10 min with 5% uranyl acetate pH 4.0, washed four times with distilled water (1 h), and then stained with 0.4% lead citrate before being observed in an JEOL 1200EX electron microscope at 80 kV (JEOL Ltd, Tokyo, Japan).

Results

WES identifies homozygous truncating mutations in *FSIP2* in four MMAF patients

Here we re-analyzed the genetic data obtained by WES from the 56 (out of 78) non-diagnosed patients (Coutton *et al.*, 2018). We searched for novel genes associated with MMAF by performing an extensive reanalysis of the remaining exomes and applying stringent technical and biological filters. We identified four patients (4/78, 5.1%) with homozygous truncating mutations in the *FSIP2* gene. The *FSIP2* gene (NM_173651) encodes a 6907-amino acid protein (Q5CZC0) and is described as one of the main genes of the flagella FS (Eddy, 2007). All identified variants: c.910delC, c.16389_16392delAATA, c.2282dupA and a complex variant c.1606_1607insTGT; 1607_1616delAAAGATTGCA are frameshift variants inserting a premature stop codon and likely abrogating the production of a functional protein. Details of the variants are provided in Fig. 2 and in Supplementary Table SIII. All the identified variants were absent from controls in the sequence databases (dbSNP, 1000 Genomes Project, NHLBI Exome Variant Server, gnomAD and in-house database), which is consistent with the expected key role of *FSIP2* in male reproduction and the negative selection of the mutations.

The *FSIP2* gene was reported in public expression databases to be strongly expressed in the testis and to be connected with the sperm flagellum (Brown *et al.*, 2003). We performed RT-qPCR experiments, which confirmed at this level of sensitivity that, in mouse and human, *FSIP2* is exclusively expressed in the testis (Supplementary Fig. S1).

In conclusion, taking into account the identification of several unrelated patients carrying homozygous *FSIP2* truncating mutations absent from all control sequences databases; the absence in these patients of other pathogenic variants in genes significantly expressed in testis and/or related to cilia/flagellum; the specific *FSIP2* expression in testes; and data from the literature reporting the involvement of AKAP4, a protein interacting with FSIP2, in human and mouse MMAF-like phenotype, we conclude that the identified *FSIP2* mutations are responsible for the MMAF phenotype of patients FSIP2_1–4.

Genotype–phenotype correlation

The morphology of patients' sperm was assessed with Papanicolaou and Harris-Schorr staining (Fig. 1). The detailed semen parameters of the four FSIP2 patients are presented in Table I and the average semen
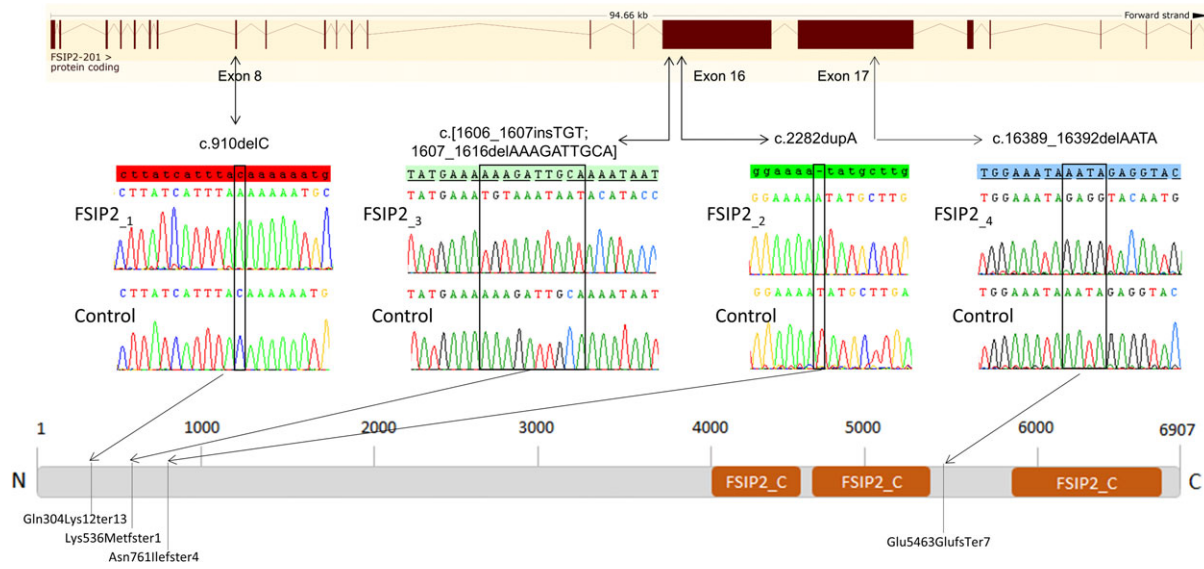
Figure 2 Location of *FSIP2* mutations in the intron–exon structure and in the protein representation. Electropherograms of Sanger sequencing for all patients with FSIP2 mutations compared to the reference sequence are reported. Orange squares show the FSIP2_C domains (fibrous sheath-interacting protein 2, C-terminal, IPR031554) as predicted by InterPro server (https://www.ebi.ac.uk/interpro/). Mutations are annotated in accordance to the Human Genome Variation Society's recommendations. According to the InterPro server, three homologous domains called FSIP2_C (C-terminus of the FSIP2 protein) are present in the C terminal part of the protein. FSIP2_C domains are present in other proteins and have been found to be repeated up to 10 times but their function is not yet known (Finn *et al.*, 2017).

parameters of the studied MMAF cohort according to the genotype are described in Table II.

As observed for the other 68 MMAF individuals of the cohort, analysis of sperm morphology from patients FSIP2_1–4 revealed very few spermatozoa with normal flagella at the expense of spermatozoa with short, absent or irregular flagella (Fig. 1). The semen parameters of the overall MMAF cohort and the detailed semen parameters of FSIP2 patients (patients FSIP2_1–4) are presented in Tables I and II. Interestingly, we observed that FSIP2 patients (FSIP2_1–4) presented a significantly lower percentage of spermatozoa with absent flagellum compared to MMAF patients with mutations in the axonemal genes *DNAH1*, *CFAP43* or *CFAP44* (*t*-test; $P < 0.05$) but no other differences were observed in the semen parameters between the two groups (Tables I and II).

FSIP2 mutations lead to severe disorganization of the FS and axonemal structure

We next studied the ultrastructure of sperm cells from patient FSIP2_4 by TEM (Fig. 3). Owing to the low sperm concentration, only a few usable images could be obtained. Longitudinal sections showed severe FS defects, which appeared completely disorganized and dysplastic (Fig. 3A and B). Outer dense fibers (ODFs) remained present whereas the mitochondrial sheath was totally absent from the midpiece and, as a consequence, the hypertrophic FS extended up to the sperm neck (Fig. 3B). Cross-sections permitting us to observe the ultrastructure of the axonemal components were also analyzed (*n* = 15). In the midpiece of spermatozoa from fertile controls, the axoneme is

surrounded by nine ODFs and the mitochondrial sheath (Fig. 3C); while in the principal piece, the axoneme is surrounded by seven ODFs and flanked by the FS composed of two longitudinal columns connected by circumferential ribs (ODFs 3 and 8 are replaced by the two longitudinal columns) (Fig. 3D). In *FSIP2* patients, 100% of the analyzed cross-sections showed a redundant and randomly arranged FS without the expected organization in longitudinal columns and circumferential ribs (Fig. 3E–H). In some principal-piece cross-sections, we counted nine ODFs indicating that the ODFs 3 and 8 were not replaced by the longitudinal columns (Fig. 3H). ODF organization was frequently altered with the presence of supernumerary or missing ODFs (Fig. 3E–G). Mitochondrial sheaths were not visible in any cross-sections. Due to limited access to patient biological material, these results, although convincing could only be obtained from a small number of sections and should be confirmed. Additional results were obtained by light microscopy which often showed a highly disorganized midpiece and IF experiments. IF experiments with anti-HSP60, which detects a mitochondrial protein located in the midpiece (Magnoni *et al.*, 2014), showed that mitochondria are still present but are strongly disorganized and scattered all along the sperm flagellum (Supplementary Fig. S2). This suggests that the absence of the mitochondrial sheath is not due to the absence of mitochondria but may be related to the impaired caudal migration of the annulus during spermiogenesis. The axoneme also showed a constant abnormal conformation with variable degrees of defects ranging from the absence of the central pair (CP) (9 + 0 conformation) to a complete disorganization (Fig. 3E–H). In addition to these obvious flagellar defects, we also observed some severe nuclear alterations, particularly in chromatin texture (data not shown).

Table I Detailed semen parameters in the four patients with the multiple morphological abnormalities of the sperm flagella phenotype and a mutation in the fibrous sheath interacting protein 2 gene.

FSIP2-mutated patients

Patient ID	Age (years)	FSIP2 mutations	Semen parameters									
			Sperm volume (ml)	Sperm concentration (10^6/ml)	Total motility (1 h)	Vitality	Normal spermatozoa	Absent flagella	Short flagella	Coiled flagella	Bent flagella	Flagella of irregular caliber
FSIP2_1	44	c.[910delC]	2.5	6.7	1	47	0	2	32	26	–	57
FSIP2_2	52	c.[2282dupA]	4.7	1.25	0	7	0	16	50	18	–	36
FSIP2_3	45	c.[1606_1607insTGT; I607_1616delAAAGATTGCA]	3.4	0.66	0	30	0	6	78	6	–	6
FSIP2_4	43	c.[16389_16392delAATA]	1.7	49.5	5	52	0	6	70	14	–	80

FSIP2, fibrous sheath interacting protein 2. Values are expressed as a percentage, unless specified otherwise.

FSIP2 mutations lead to the absence of AKAP4 protein and an altered distribution of the axonemal components

Despite repeated attempts, no antibodies specifically recognizing FSIP2 in human sperm cells could be obtained, precluding the immuno-detection of FSIP2 protein on sperm samples from control individuals and its potential absence in FSIP2_1–4 patients. We therefore decided to analyze the distribution of various proteins of the sperm flagellum, and in particular of AKAP4, a protein described to localize to the FS and to directly interact with FSIP2 (Brown *et al.*, 2003). We performed some IF assays on sperm cells and observed that the AKAP4 staining was totally absent from patient FSIP2_3 and FSIP2_4 whereas AKAP4 immunostaining was strong in the principal piece of the sperm flagellum of control sperm cells from fertile individual (Fig. 4). In order to determine if the loss of AKAP4 was a constant feature of the MMAF phenotype, we analyzed MMAF patients carrying mutations in *CFAP43*, *CFAP44* and *DNAH1*. In these patients, AKAP4 immunostaining was comparable with that observed in fertile controls (Fig. 4), indicating that the molecular structure of the FS was not as severely altered in the sperm from MMAF patients with mutations in axoneme-related genes. We decided to further investigate the flagellum structure of FSIP2 patients by performing immunostaining with antibodies targeting different axonemal proteins. We analyzed the sperm associated antigen 6 (SPAG6), a component of the CP complex. In a fertile control, we observed that SPAG6 staining was concentrated in the principal piece of the spermatozoa whereas staining was absent or strongly reduced in FSIP2-mutated patients with an abnormal and diffuse pattern concentrated on the flagellum's proximal part (Supplementary Fig. S3A). Moreover, staining of dynein axonemal heavy chain 5 (DNAH5) and dynein axonemal light intermediate chain 1 (DNALI1), two proteins located in the outer dynein arms and inner dynein arms, respectively, were absent in FSIP2_3 and FSIP2_4 patients demonstrating that the whole axonemal structure was strongly affected by the presence of the FSIP2 mutations (Supplementary Fig. S3B, C).

Discussion

The study presented here allowed us to demonstrate that the absence of functional FSIP2, a protein of the sperm flagella FS, induced a MMAF phenotype. Logically, TEM analyses of sperm from our FSIP2 patients revealed a severe dysplasia of the FS, which appeared extremely disorganized and hypertrophic. Such FS defects were previously reported and studied in patients with a MMAF-like phenotype initially described as DFS (Chemes *et al.*, 1987; Chemes and Rawe, 2003, 2010; Chemes and Alvarez Sedo, 2012). These FS defects do not seem to be as marked in sperm cells from other MMAF patients with mutations in the three axonemal genes *DNAH1*, *CFAP43* and *CFAP44* (Ben Khelifa *et al.*, 2014; Coutton *et al.*, 2015, 2018; Tang *et al.*, 2017). The FS is a cytoskeletal structure located in the principle piece of the sperm flagellum, which seems to be unique to amniote sperm flagellum (Fawcett, 1970). This is consistent with our expression data showing a specific expression of *FSIP2* in the testis with no detectable expression in the other ciliated tissues (Supplementary Fig. S1). In the principal piece, the FS is formed by two longitudinal columns connected by circumferential ribs (Eddy *et al.*, 2003). The FS is believed to serve as a scaffold for numerous proteins including glycolytic enzymes or signaling protein

Table II Average semen parameters in patients mutated in *FSIP2*, in other xonemal-associated genes, and for the 78 subjects with multiple morphological abnormalities of the sperm flagella in the study.

Semen parameters	MMAF with *FSIP2* mutations $n = 4$	MMAF other mutations$^\$$ $n = 22$	Overall MMAF $n = 78$	Reference limits[%]
Mean age (years)	46 ± 4	39.8 ± 7	41.6 ± 7.7	NA
	(n′ = 4)	(n′ = 21)	(n′ = 77)	
Sperm volume (ml)	3.1 ± 1.3	3.4 ± 1.2	3.5 ± 1.4	1.5 (1.4–1.7)
	(n′ = 4)	(n′ = 20)	(n′ = 75)	
Sperm concentration (10^6/ml)	14.5 ± 23.5	20.1 ± 18.8	25.6 ± 32.1	15 (12–16)
	(n′ = 4)	(n′ = 20)	(n′ = 75)	
Total motility (1 h)	1.5 ± 2.4	0.7 ± 2.4	3.9 ± 5.6	40 (38–42)
	(n′ = 4)	(n′ = 21)	(n′ = 76)	
Vitality	34 ± 20.3	50.5 ± 22.7	52.7 ± 20	58 (55–63)
	(n′ = 4)	(n′ = 19)	(n′ = 72)	
Normal spermatozoa	0 ± 0	0.5 ± 2.3	1.6 ± 2.7	23 (20–26)
	(n′ = 4)	(n′ = 20)	(n′ = 61)	
Absent flagella	7.5 ± 5.9*	28.1 ± 14.4	20.7 ± 15.7	5 (4–6)
	(n′ = 4)	(n′ = 15)	(n′ = 66)	
Short flagella	57.5 ± 20.6	57.1 ± 27.9	43.7 ± 27.3	1 (0–2)
	(n′ = 4)	(n′ = 19)	(n′ = 72)	
Coiled flagella	16 ± 8.3	10.4 ± 6.6	12.8 ± 9.4	17 (15–19)
	(n′ = 4)	(n′ = 16)	(n′ = 69)	
Bent flagella	NA	8.7 ± 5.8	4.2 ± 8.4	13 (11–15)
		(n′ = 6)	(n′ = 26)	
Flagella of irregular caliber	44.8 ± 31.5	27.9 ± 19.4	31.7 ± 25.1	2 (1–3)
	(n′ = 4)	(n′ = 15)	(n′ = 67)	

MMAF, multiple morphological abnormalities of the sperm flagella.
Values are expressed as a percentage, unless specified otherwise. Values are mean ± SD; *n* = total number of patients in each group; *n′* = number of patients used to calculate the average based on available data; NA, not available.
$^\$$Other mutations correspond to patients with mutations in cilia and flagella associated protein 43 (*CFAP43*) and 44 (*CFAP44*) and dynein axonemal heavy chain 1 (*DNAH1*) genes, according to Coutton *et al.* (2018).
[%]Reference limits (fifth centiles and their 95% CI) according to the World Health Organization standards (Cooper *et al.*, 2010) and the distribution range of morphologically normal spermatozoa observed in 926 fertile individuals (Auger *et al.*, 2016).
*Significant *P* < 0.05 (Student's *t*-test).

and to play a role in the regulation of sperm motility but also in sperm maturation, capacitation and hyperactivation (Eddy *et al.*, 2003; Eddy, 2007). An important part of the enzymatic and energy metabolism of the principal piece is likely regulated by the cAMP-dependent protein kinase A (PKA) which is anchored in the FS through different AKAPs (Carr and Newell, 2007). AKAPs are a family composed of around 50 scaffold proteins which confine various enzymes including kinases, phosphatases and phosphodiesterases and their corresponding enzymatic activities to specific intracellular locations (Kumar *et al.*, 2017). In sperm, six AKAPs have been identified, three of which (AKAP3, AKAP4 and AKAP14) are located in the FS (Fiedler *et al.*, 2008). FSIP2 was shown to bind to AKAP4, the most abundant AKAP of the FS, which was described to be important for completing FS assembly (Brown *et al.*, 2003; Nipper *et al.*, 2006). Furthermore, the region where FSIP2 likely docks onto AKAP4 encompasses the RIa/RIIa-dual domain, which is the docking domain of PKA onto the AKAP proteins, suggesting that FSIP2 could have a role in regulating PKA anchoring to AKAP4 (Turner *et al.*, 1998; Brown *et al.*, 2003; Welch

et al., 2010). Here we showed that in FSIP2-deficient patients, AKAP4 was absent from the sperm flagellum contrary to what was observed in the other patients with a similar phenotype owing to mutations in axonemal-associated MMAF genes (Fig. 4). Interestingly, it has been previously reported that AKAP4-deficient mice also had shortened flagella with an irregular diameter of the principal piece (Miki *et al.*, 2002) as observed in our FSIP2-mutated patients (Fig. 1). In addition, the only patient reported with a partial deletion of *AKAP4* (Baccetti *et al.*, 2005), also presented spermatozoa with extremely short tails and severe FS dysplasia.

In addition to the severe abnormalities of the peri-axonemal structures described above, sperm from patients with *FSIP2* mutations also displayed some axonemal anomalies including the absence of the CP and of all the inner/outer dynein arms (Figs 3 and 4). Such axonemal defects were also described in sperm cells from patients described as DFS (Chemes and Rawe, 2003, 2010). Moreover, when discussing the phenotype of their *AKAP4* deleted patient, Baccetti *et al.* (2005) also reported that their patient's sperm had an altered axonemal structure
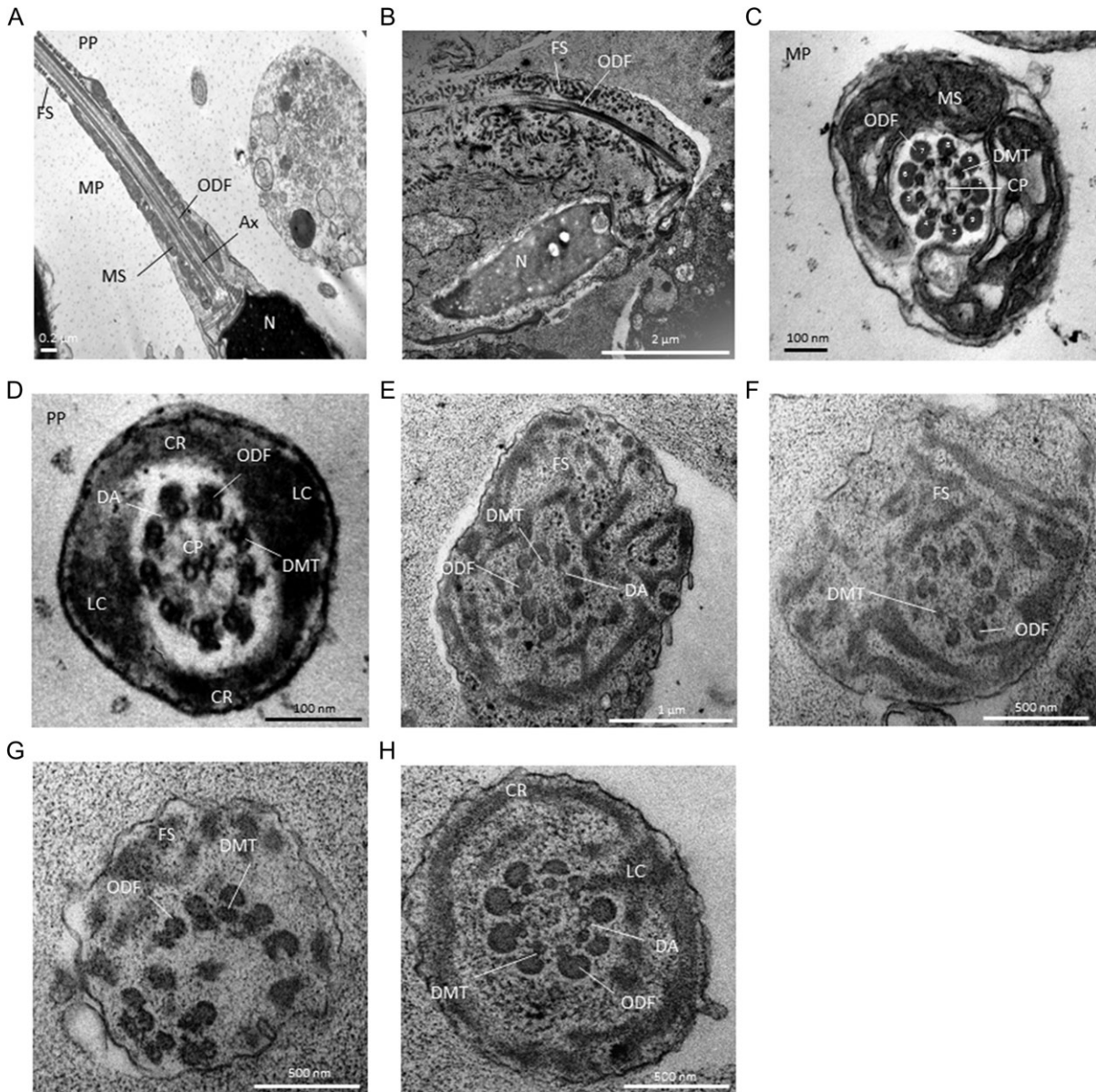
Figure 3 Transmission electron microscopy analyses of sperm cells from a control subject (**A**, **C**, **D**) and patient FSIP2_4 (**B**, **E**–**H**). (A) Longitudinal sections of sperm flagellum from control. In the midpiece (MP), outer dense fibers (ODF) are found longitudinally between the mitochondrial sheath (MS) and the axoneme (Ax). The fibrous sheath (FS) is found in the principal piece (PP). N, nucleus. (B) Longitudinal sections of sperm flagellum from patient FSIP2_4. We notice an abnormal flagellum with the FS which appears severly disorganized and extends up to the sperm neck. ODFs remains present whereas the MS is totally absent from the midpiece likely due to an abnormal migration of the annulus. The central axoneme is not clearly visible. (C) Cross-sections of the MP in a control. The axoneme is surrounded by nine ODFs and the MS. The axoneme is composed of nine peripheral microtubules doublets (DMTs) and a central pair (CP) of singlet microtubules. (D) Cross-sections of the PP from a fertile control. The axoneme is surrounded by seven ODFs and by the FS composed of two longitudinal columns (LC) connected by circumferential ribs (CR). DA, dynein arms. (E–H) Cross-sections of sperm flagellum from patient FSIP2_4. The FS is dysplastic, thickened and dramatically disorganized with randomly oriented fibers (E–G). When the CR seem present, we observed only one nascent and abnormal LC adjacent to doublets 3 or 8 (H). Various axonemal anomalies can be observed including the lack of the CP (E, F, H) or complete axonemal desorganization (G). Alterations of ODFs is also seen with surpernumeray (E), missing (F) or fully disorganized ODFs (G). DA are rarely visible (E, H).

with missing dynein arms and CP. They however did not present any sperm tail cross-sections, making a reliable comparison with our patients difficult. Since the axoneme is assembled soon after the completion of meiosis and appears before the FS (Horowitz *et al.*, 2005), we can presume that these axonemal defects are secondary to FS misassembly or disorganization. This assumption is supported by studies on testicular biopsies from DFS patients showing that the phenotype arises during late spermiogenesis (Ross *et al.*, 1973; Barthelemy *et al.*,
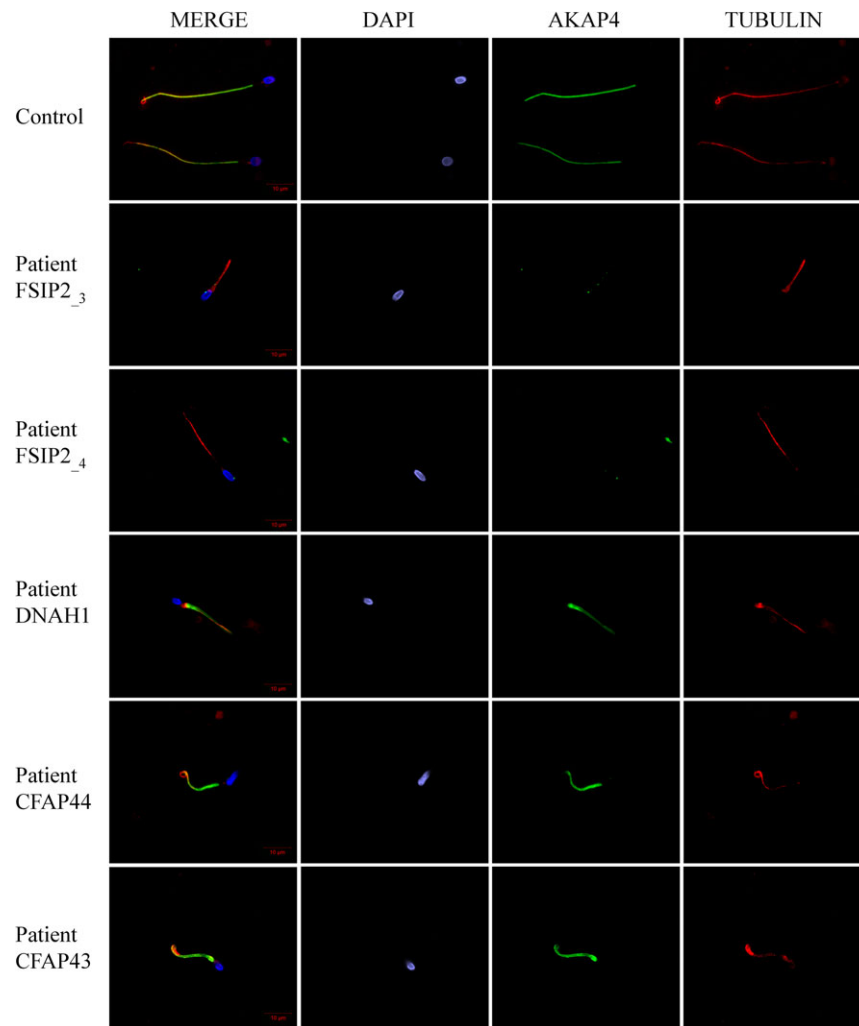
Figure 4 A-kinase anchoring protein 4 is absent in sperm cells from patients with *FSIP2* mutations. Sperm cells from a fertile control, the two patients FSIP2_3 and FSIP2_4, and three other patients mutated in dynein axonemal heavy chain 1 (*DNAH1*) gene, and in the cilia and flagella associated protein 43 (*CFAP43*) and 44 (*CFAP44*) genes, respectively, were stained with anti-A-kinase anchoring protein 4 (AKAP4: green) and anti-acetylated tubulin (red) antibodies. DNA was counterstained with DAPI showing sperm nuclear DNA (blue). The AKAP4 immunostaining is concentrated in the PP of the spermatozoa from the fertile control and the three patients mutated in *DNAH1, CFAP43* and *CFAP44*. Conversely, AKAP4 staining is absent in sperm from the two patients FSIP2_3 and FSIP2_4. Scale bar 10 μm.

1990; Rawe *et al.*, 2002; Chemes and Rawe, 2010). Altogether these elements clearly indicate that the patients whose MMAF is caused by *FSIP2* mutations present a DFS ultrastructural phenotype.

Absence of FSIP2 and consequently of AKAP4 could impede the correct localization of functionally important FS-associated proteins that are critical for the maintenance of sperm function and structure, such as PKA or glycolytic enzymes (Miki *et al.*, 2002; de Boer *et al.*, 2015). Additionally, the important disorganization of the FS and the failure to form the longitudinal columns may also alter the direct interaction of microtubule doublets (DMTs) 3 and 8 with the FS in the principal piece and weaken the stability of the axonemal structures leading to the total destabilization of the axoneme. We have just demonstrated that CFAP43 and CFAP44 likely link the axoneme with the extra-axonemal components (Coutton *et al.*, 2018). This suggests that most of the flagellar structures are tightly connected and defects in any

of these structures may alter the whole process of flagellar genesis and produce a MMAF phenotype. Intriguingly, we observed that the sperm phenotype induced by the presence of *FSIP2* mutations is more severe than what was described for *Akap4* mutant mice (Miki *et al.*, 2002), where only the FS was described as being affected. This could indicate that FSIP2 is not only a structural protein of the FS but that it may be involved in the intraflagellar transport of several components, potentially including AKAP4. Further studies are now required to define the role of the different proteins found to be associated with a MMAF phenotype, and to identify and characterize sub-phenotypes induced by the different molecular defects. Overall, this demonstrates the crucial importance of FSIP2 in maintaining the whole structure and function of the sperm flagellum.

WES analysis permitted the identification of four *FSIP2* loss of function variants. All were indels including nucleotide deletions,

duplications or insertions. No obvious phenotype differences were observed among these four patients, concordant with the fact that all identified mutations are expected to induce the production of a truncated non-functional protein. Interestingly we noted that patients with *FSIP2* mutations presented a significant lower rate of spermatozoa with absent flagella compared to patients with an identified mutation in other MMAF genes suggesting that *FSIP2* mutations might not alter the head-flagella junction as severely as mutations in axonemal-related genes. Moreover, although not statistically significant, FSIP2 patients had a higher rate of flagella with an irregular diameter, which is consistent with the overabundance and disorganization of the FS (Chemes and Rawe, 2010). Several questions remain concerning the prognosis of ICSI using sperm cells from *FSIP2* patients. Successful application of ICSI in patients with MMAF has been previously described, including patients carrying mutations in *DNAH1* (Olmedo *et al.*, 2000; Chemes and Rawe, 2003; Chemes and Alvarez Sedo, 2012; Dávila Garza and Patrizio, 2013; Coutton *et al.*, 2015; Wambergue *et al.*, 2016). However, so far it remains difficult to predict the prognosis for patients carrying FSIP mutations, as ICSI success rates have been described to be influenced by the type of ultrastructural flagellar defects (Mitchell *et al.*, 2006; Fauque *et al.*, 2009; Coutton *et al.*, 2015). Additional correlation studies should now be performed to take into account the individual genotypes in the counseling of MMAF patients.

A previous study of the cohort presented here permitted the identification of 22 patients (28.2%) with mutations in *DNAH1*, *CFAP43* and *CFAP44* (Coutton *et al.*, 2018) and two patients with *CFAP69* mutations (Dong *et al.*, 2018). In the present study, we identified four additional patients with *FSIP2* mutations and established *FSIP2* as a new recurrent genetic cause of MMAF present in more than 5% of our cohort. The overall rate of a positive molecular diagnosis for this cohort is therefore 36% (28/78) which is close to the diagnosis rate found in other diseases with heterogeneous genetic etiologies (Farwell *et al.*, 2015; Fogel *et al.*, 2016). Our data thus demonstrate the clinical utility of WES for the identification of genetic causes responsible for male infertility due to a MMAF phenotype. In-depth bioinformatic analyses of WES data from the remaining 50 undiagnosed individuals from this cohort, together with the inclusion of additional MMAF patients, will likely improve the diagnosis yield and bring to light other rare genetic defects inducing a MMAF phenotype.

Supplementary data

Supplementary data are available at *Human Reproduction* online.

Acknowledgements

We thank all patients and control individuals for their participation.

Authors' roles

C.C., P.F.R., C.A., M.B. and A.T. analyzed the data and wrote the article; T.K., Z.K., N.T.M., M.B., A.A.Y., P.F.R. and C.C. performed and analyzed genetic data; G.M., A.S. performed IF experiments; K.P.G., A.B. and G.M. performed EM experiments, sperm analyses; R.Z., V.S. provided clinical samples and data; C.C., P.F.R., C.A. and G.M. designed the study, supervised all molecular laboratory work, had full access to all of the data in the study and takes responsibility for the integrity of the data and its accuracy. All authors contributed to the report.

Conflict of interest

The authors have declared that no conflict of interest exists.

References

1000 Genomes Project Consortium, Abecasis GR, Auton A, Brooks LD, DePristo MA, Durbin RM, Handsaker RE, Kang HM, Marth GT, McVean GA. An integrated map of genetic variation from 1,092 human genomes. *Nature* 2012;**491**:56–65.

Adzhubei IA, Schmidt S, Peshkin L, Ramensky VE, Gerasimova A, Bork P, Kondrashov AS, Sunyaev SR. A method and server for predicting damaging missense mutations. *Nat Methods* 2010;**7**:248–249.

Amiri-Yekta A, Coutton C, Kherraf Z-E, Karaouzène T, Le Tanno P, Sanati MH, Sabbaghian M, Almadani N, Sadighi Gilani MA, Hosseini SH *et al.* Whole-exome sequencing of familial cases of multiple morphological abnormalities of the sperm flagella (MMAF) reveals new DNAH1 mutations. *Hum Reprod* 2016;**31**:2872–2880.

Auger J, Jouannet P, Eustache F. Another look at human sperm morphology. *Hum Reprod* 2016;**31**:10–23.

Baccetti B, Collodel G, Estenoz M, Manca D, Moretti E, Piomboni P. Gene deletions in an infertile man with sperm fibrous sheath dysplasia. *Hum Reprod* 2005;**20**:2790–2794.

Barthelemy C, Tharanne MJ, Lebos C, Lecomte P, Lansac J. Tail stump spermatozoa: morphogenesis of the defect. An ultrastructural study of sperm and testicular biopsy. *Andrologia* 1990;**22**:417–425.

Ben Khelifa M, Coutton C, Zouari R, Karaouzène T, Rendu J, Bidart M, Yassine S, Pierre V, Delaroche J, Hennebicq S *et al.* Mutations in DNAH1, which encodes an inner arm heavy chain dynein, lead to male infertility from multiple morphological abnormalities of the sperm flagella. *Am J Hum Genet* 2014;**94**:95–104.

Brown PR, Miki K, Harper DB, Eddy EM. A-kinase anchoring protein 4 binding proteins in the fibrous sheath of the sperm flagellum. *Biol Reprod* 2003;**68**:2241–2248.

Carr DW, Newell AEH. The role of A-kinase anchoring proteins (AKaps) in regulating sperm function. *Soc Reprod Fertil Suppl* 2007;**63**:135–141.

Chemes HE. Phenotypes of sperm pathology: genetic and acquired forms in infertile men. *J Androl* 2000;**21**:799–808.

Chemes HE, Alvarez Sedo C. Tales of the tail and sperm head aches: changing concepts on the prognostic significance of sperm pathologies affecting the head, neck and tail. *Asian J Androl* 2012;**14**:14–23.

Chemes HE, Brugo S, Zanchetti F, Carrere C, Lavieri JC. Dysplasia of the fibrous sheath: an ultrastructural defect of human spermatozoa associated with sperm immotility and primary sterility. *Fertil Steril* 1987;**48**:664–669.

Chemes HE, Olmedo SB, Carrere C, Oses R, Carizza C, Leisner M, Blaquier J. Ultrastructural pathology of the sperm flagellum: association between flagellar pathology and fertility prognosis in severely astheno-zoospermic men. *Hum Reprod* 1998;**13**:2521–2526.

Chemes EH, Rawe YV. Sperm pathology: a step beyond descriptive morphology. Origin, characterization and fertility potential of abnormal sperm phenotypes in infertile men. *Hum Reprod Update* 2003;**9**: 405–428.

Chemes HE, Rawe VY. The making of abnormal spermatozoa: cellular and molecular mechanisms underlying pathological spermiogenesis. *Cell Tissue Res* 2010;**341**:349–357.

Cooper TG, Noonan E, Eckardstein S, von, Auger J, Baker HWG, Behre HM, Haugen TB, Kruger T, Wang C, Mbizvo MT *et al*. World Health Organization reference values for human semen characteristics. *Hum Reprod Update* 2010;**16**:231–245.

Coutton C, Escoffier J, Martinez G, Arnoult C, Ray PF. Teratozoospermia: spotlight on the main genetic actors in the human. *Hum Reprod Update* 2015;**21**:455–485.

Coutton C, Vargas AS, Amiri-Yekta A, Kherraf Z-E, Ben Mustapha SF, Le Tanno P, Wambergue-Legrand C, Karaouzène T, Martinez G, Crouzy S *et al*. Mutations in CFAP43 and CFAP44 cause male infertility and flagel-lum defects in Trypanosoma and human. *Nat Commun* 2018;**9**:686.

de Boer P, de Vries M, Ramos L. A mutation study of sperm head shape and motility in the mouse: lessons for the clinic. *Andrology* 2015;**3**: 174–202.

Dong FN, Amiri-Yekta A, Martinez G, Saut A, Tek J, Stouvenel L, Lorès P, Karaouzène T, Thierry-Mieg N, Satre V *et al*. Absence of CFAP69 causes male infertility due to multiple morphological abnormalities of the flagella in human and mouse. *Am J Hum Genet* 2018;**102**:636–648.

Dávila Garza SA, Patrizio P. Reproductive outcomes in patients with male infertility because of Klinefelter's syndrome, Kartagener's syndrome, round-head sperm, dysplasia fibrous sheath, and 'stump' tail sperm: an updated literature review. *Curr Opin Obstet Gynecol* 2013;**25**:229–246.

Eddy EM. The scaffold role of the fibrous sheath. *Soc Reprod Fertil Suppl* 2007;**65**:45–62.

Eddy EM, Toshimori K, O'Brien DA. Fibrous sheath of mammalian sperm-atozoa. *Microsc Res Tech* 2003;**61**:103–115.

Escalier D, David G. Pathology of the cytoskeleton of the human sperm flagellum: axonemal and peri-axonemal anomalies. *Biol Cell* 1984;**50**: 37–52.

Farwell KD, Shahmirzadi L, El-Khechen D, Powis Z, Chao EC, Tippin Davis B, Baxter RM, Zeng W, Mroske C, Parra MC *et al*. Enhanced utility of family-centered diagnostic exome sequencing with inheritance model-based analysis: results from 500 unselected families with undiagnosed genetic conditions. *Genet Med* 2015;**17**:578–586.

Fauque P, Albert M, Serres C, Viallon V, Davy C, Epelboin S, Chalas C, Jouannet P, Patrat C. From ultrastructural flagellar sperm defects to the health of babies conceived by ICSI. *Reprod Biomed Online* 2009;**19**: 326–336.

Fawcett DW. A comparative view of sperm ultrastructure. *Biol Reprod Suppl* 1970;**2**:90–127.

Fiedler SE, Bajpai M, Carr DW. Identification and characterization of RHOA-interacting proteins in bovine spermatozoa. *Biol Reprod* 2008;**78**: 184–192.

Finn RD, Attwood TK, Babbitt PC, Bateman A, Bork P, Bridge AJ, Chang H-Y, Dosztányi Z, El-Gebali S, Fraser M *et al*. InterPro in 2017-beyond protein family and domain annotations. *Nucleic Acids Res* 2017;**45**: D190–D199.

Fogel BL, Lee H, Strom SP, Deignan JL, Nelson SF. Clinical exome sequen-cing in neurogenetic and neuropsychiatric disorders. *Ann N Y Acad Sci* 2016;**1366**:49–60.

Horowitz E, Zhang Z, Jones BH, Moss SB, Ho C, Wood JR, Wang X, Sammel MD, Strauss JF. Patterns of expression of sperm flagellar genes: early expression of genes encoding axonemal proteins during the sper-matogenic cycle and shared features of promoters of genes encoding central apparatus proteins. *Mol Hum Reprod* 2005;**11**:307–317.

Inaba K. Molecular architecture of the sperm flagella: molecules for motility and signaling. *Zoolog Sci* 2003;**20**:1043–1056.

Inaba K. Molecular basis of sperm flagellar axonemes: structural and evolu-tionary aspects. *Ann N Y Acad Sci* 2007;**1101**:506–526.

Inaba K. Sperm flagella: comparative and phylogenetic perspectives of pro-tein components. *Mol Hum Reprod* 2011;**17**:524–538.

Kumar P, Henikoff S, Ng PC. Predicting the effects of coding non-synonymous variants on protein function using the SIFT algorithm. *Nat Protoc* 2009;**4**:1073–1081.

Kumar V, Jagadish N, Suri A. Role of A-kinase anchor protein (AKAP4) in growth and survival of ovarian cancer cells. *Oncotarget* 2017;**8**: 53124–53136.

Lehti MS, Sironen A. Formation and function of sperm tail structures in association with sperm motility defects. *Biol Reprod* 2017;**97**:522–536.

Lek M, Karczewski KJ, Minikel EV, Samocha KE, Banks E, Fennell T, O'Donnell-Luria AH, Ware JS, Hill AJ, Cummings BB *et al*. Analysis of protein-coding genetic variation in 60,706 humans. *Nature* 2016;**536**: 285–291.

Livak KJ, Schmittgen TD. Analysis of relative gene expression data using real-time quantitative PCR and the 2(-Delta Delta C(T)) Method. *Methods San Diego Calif* 2001;**25**:402–408.

Magnoni R, Palmfeldt J, Hansen J, Christensen JH, Corydon TJ, Bross P. The Hsp60 folding machinery is crucial for manganese superoxide dis-mutase folding and function. *Free Radic Res* 2014;**48**:168–179.

McLaren W, Gil L, Hunt SE, Riat HS, Ritchie GRS, Thormann A, Flicek P, Cunningham F. The Ensembl variant effect predictor. *Genome Biol* 2016; **17**:122.

Miki K, Willis WD, Brown PR, Goulding EH, Fulcher KD, Eddy EM. Targeted disruption of the Akap4 gene causes defects in sperm flagellum and motility. *Dev Biol* 2002;**248**:331–342.

Mitchell V, Rives N, Albert M, Peers M-C, Selva J, Clavier B, Escudier E, Escalier D. Outcome of ICSI with ejaculated spermatozoa in a series of men with distinct ultrastructural flagellar abnormalities. *Hum Reprod Oxf Engl* 2006;**21**:2065–2074.

Nipper RW, Jones BH, Gerton GL, Moss SB. Protein domains govern the intracellular distribution of mouse sperm AKAP4. *Biol Reprod* 2006;**75**: 189–196.

Olmedo SB, Rawe VY, Nodar FN, Galaverna GD, Acosta AA, Chemes HE. Pregnancies established through intracytoplasmic sperm injection (ICSI) using spermatozoa with dysplasia of fibrous sheath. *Asian J Androl* 2000;**2**:125–130.

Rawe VY, Galaverna GD, Acosta AA, Olmedo SB, Chemes HE. Incidence of tail structure distortions associated with dysplasia of the fibrous sheath in human spermatozoa. *Hum Reprod* 2001;**16**:879–886.

Rawe VY, Terada Y, Nakamura S, Chillik CF, Olmedo SB, Chemes HE. A pathology of the sperm centriole responsible for defective sperm aster formation, syngamy and cleavage. *Hum Reprod* 2002; **17**:2344–2349.

Ray PF, Toure A, Metzler-Guillemain C, Mitchell MJ, Arnoult C, Coutton C. Genetic abnormalities leading to qualitative defects of sperm morph-ology or function. *Clin Genet* 2017;**91**:217–232.

Ross A, Christie S, Edmond P. Ultrastructural tail defects in the spermato-zoa from two men attending a subfertility clinic. *J Reprod Fertil* 1973;**32**: 243–251.

Satir P, Christensen ST. Structure and function of mammalian cilia. *Histochem Cell Biol* 2008;**129**:687–693.

SEQC/MAQC-III Consortium. A comprehensive assessment of RNA-seq accuracy, reproducibility and information content by the Sequencing Quality Control Consortium. *Nat Biotechnol* 2014;**32**:903–914.

Sha Y, Yang X, Mei L, Ji Z, Wang X, Ding L, Li P, Yang S. DNAH1 gene mutations and their potential association with dysplasia of the sperm fibrous sheath and infertility in the Han Chinese population. *Fertil Steril* 2017;**107**:1312–1318.e2.

Tang S, Wang X, Li W, Yang X, Li Z, Liu W, Li C, Zhu Z, Wang L, Wang J et al. Biallelic mutations in CFAP43 and CFAP44 cause male infertility with multiple morphological abnormalities of the sperm flagella. *Am J Hum Genet* 2017;**100**:854–864.

Turner RM, Johnson LR, Haig-Ladewig L, Gerton GL, Moss SB. An X-linked gene encodes a major human sperm fibrous sheath protein, hAKAP82. Genomic organization, protein kinase A-RII binding, and distribution of the precursor in the sperm tail. *J Biol Chem* 1998;**273**: 32135–32141.

Turner RM, Musse MP, Mandal A, Klotz K, Jayes FC, Herr JC, Gerton GL, Moss SB, Chemes HE. Molecular genetic analysis of two human sperm fibrous sheath proteins, AKAP4 and AKAP3, in men with dysplasia of the fibrous sheath. *J Androl* 2001;**22**:302–315.

Wambergue C, Zouari R, Fourati Ben Mustapha S, Martinez G, Devillard F, Hennebicq S, Satre V, Brouillet S, Halouani L, Marrakchi O et al. Patients with multiple morphological abnormalities of the sperm flagella due to DNAH1 mutations have a good prognosis following intracytoplasmic sperm injection. *Hum Reprod* 2016;**31**:1164–1172.

Wang Y, Yang J, Jia Y, Xiong C, Meng T, Guan H, Xia W, Ding M, Yuchi M. Variability in the morphologic assessment of human sperm: use of the strict criteria recommended by the World Health Organization in 2010. *Fertil Steril* 2014;**101**:945–949.

Welch EJ, Jones BW, Scott JD. Networking with AKAPs: context-dependent regulation of anchored enzymes. *Mol Interv* 2010;**10**: 86–97.